university of groningen

University Medical Center Groningen

University of Groningen

The influence of the surface topography on the magnetization dynamics in soft magnetic thin films

Craus, C. B.; Palasantzas, G.; Chezan, A. R.; De Hosson, J. Th. M.; Boerma, D. O.; Niesen, L.

Published in:
Journal of Applied Physics

DOI:
10.1063/1.1819998

IMPORTANT NOTE: You are advised to consult the publisher's version (publisher's PDF) if you wish to cite from it. Please check the document version below.

Document Version
Publisher's PDF, also known as Version of record

Publication date:
2005

Link to publication in University of Groningen/UMCG research database

Citation for published version (APA):
Craus, C. B., Palasantzas, G., Chezan, A. R., De Hosson, J. T. M., Boerma, D. O., & Niesen, L. (2005). The influence of the surface topography on the magnetization dynamics in soft magnetic thin films. *Journal of Applied Physics*, *97*(1), 013904-1 - 013904-8. [013904]. https://doi.org/10.1063/1.1819998

Copyright
Other than for strictly personal use, it is not permitted to download or to forward/distribute the text or part of it without the consent of the author(s) and/or copyright holder(s), unless the work is under an open content license (like Creative Commons).

The publication may also be distributed here under the terms of Article 25fa of the Dutch Copyright Act, indicated by the “Taverne” license. More information can be found on the University of Groningen website: https://www.rug.nl/library/open-access/self-archiving-pure/taverne-amendment.

Take-down policy
If you believe that this document breaches copyright please contact us providing details, and we will remove access to the work immediately and investigate your claim.

Downloaded from the University of Groningen/UMCG research database (Pure): http://www.rug.nl/research/portal. For technical reasons the number of authors shown on this cover page is limited to 10 maximum.

HTML ABSTRACT + LINKS

The influence of the surface topography on the magnetization dynamics in soft magnetic thin films

C. B. Craus[a]
Systems and Materials for Information Storage, Microelectronics, Sensors, and Actuators+Research Institute, P.O. Box 217, 7500 AE Enschede, The Netherlands

G. Palasantzas, A. R. Chezan, J. Th. M. De Hosson, D. O. Boerma, and L. Niesen
Department of Applied Physics, Materials Science Center, University of Groningen, Nijenborgh 4, 9747 AG Groningen, The Netherlands

(Received 21 June 2004; accepted 29 September 2004; published online 16 December 2004)

In this work we study the influence of surface roughness on the magnetization dynamics of soft magnetic nanocrystalline Fe–Zr–N thin films deposited (under identical conditions) onto a Si oxide, a thin polymer layer, and a thin Cu layer. The substrate temperature during deposition was approximately −25 °C ensuring a nanocrystalline state. The demagnetizing factors due to sample roughness were calculated based on atomic force microscopy (AFM) analysis of the surface topography. A clear correlation between sample roughness and the width of the high-frequency response is observed. The local random demagnetizing field created by the nanocrystalline structure and the surface topography is responsible for the positive shift of the ferromagnetic resonance frequency. In addition, a pronounced effect of line broadening is induced by the surface topography at large wavelengths. Finally, we show a good agreement between the values of the average demagnetizing field $4\pi NM_S$ as calculated from the AFM scans, and the values calculated from the frequency-dependent complex permeability measurements. © *2005 American Institute of Physics*.
[DOI: 10.1063/1.1819998]

I. INTRODUCTION

The development of technologies related to the magnetic recording industry and the spread of wireless communication systems is an important incentive to focus on magnetic materials, which can be used in high-frequency applications.[1,2] Depending on the application, the requirements, which must be satisfied by these materials, can vary considerably. For instance, in order to improve the design of a high-frequency inductor we can use a soft magnetic material with high ferromagnetic resonance (FMR) frequency. A narrow FMR line and a high real component of the magnetic permeability are in this case desirable. Somewhat different properties must be satisfied by the materials, which are used for band stop filters which depend on the absorption of microwave power at FMR frequency; the position and the width of the FMR line must be adjustable depending on the working frequency range. Therefore it is desirable to obtain a magnetic material, which can be used for a large range of frequencies. The high-frequency properties of this material will be artificially modified changing the extrinsic parameters of the samples.

In order to have a "tunable" magnetic material, the magnetocrystalline anisotropy has to be minimized. This can be performed by choosing a nanocrystalline structure with random orientation of the grains.[3,4] An important factor is also the saturation magnetization M_S. In almost all high-frequencies applications involving a ferromagnetic material, an increase of M_S leads to an improvement of the physical property of interest. For example we have (i) for an inductor, a higher M_S increases the inductance and the frequency range, and (ii) for a stop band filter higher M_S means higher power absorption.

At any rate, in this article we present a study of the high-frequency response of Fe–Zr–N thin films with a nanocrystalline structure and uniaxial induced anisotropy, where we concentrate on the topography variation of the substrate on which the films are deposited. Indeed, it is shown that substrate roughness induces significant changes of the magnetization dynamics. The FMR frequency distribution is very broad and the average FMR frequency is shifted upward corresponding to an extra field of about 35 Oe for the sample deposited on the roughest substrate. Finally, we discuss the origin of both the broadening and the frequency shift.

II. EXPERIMENT

The deposition method used for the production of the samples was dc reactive sputtering in an $Ar+N_2$ gas mixture. We have kept the same sputtering parameters for all samples used in this investigation. The target material was a Fe–Zr alloy with a Zr concentration of only 1%. This small amount of Zr has the role of increasing the nitrogen uptake and may act also as a thermal stabilizer in subsequent treatments. Here, only the first Zr-related property was considered for this study, since no thermal treatments were performed. The film thickness was fixed at 110 nm. Another important factor in sample deposition was the temperature of the substrate. All samples were produced at temperatures below −20 °C producing grain sizes around 2 nm (see Table I). More details about this deposition technique are given elsewhere.[5,6]

[a]Author to whom correspondence should be addressed; present address: MESA+Research Institute, 7500 AE Enschede, The Netherlands; electronic mail: c.b.Craus@el.utwente.nl

0021-8979/2005/97(1)/013904/8/$22.50 © 2005 American Institute of Physics

Downloaded 05 Oct 2006 to 129.125.25.39. Redistribution subject to AIP license or copyright, see http://jap.aip.org/jap/copyright.jsp

TABLE I. Structural parameters of the samples; w is the rms roughness amplitude.

Sample name	A	B	C
Substrate	Si(100)	Organic	Cu (300 nm)
Dep. Temp. (°C)	−27	−32	−24
Grain size (nm)	2	2	~2
N (at. %)	16.1	14.5	~15
w (nm)	0.3	2.3	5.1

In order to change the topography of the samples, we have used the following substrates: (i) Si oxide, (ii) Si covered with a thin organic layer, and (iii) Si oxide covered with a 300-nm Cu layer. The second substrate was prepared by applying a uniform layer of dinitro cellulose in a solution of amilacetate and acetone (colodium) with a thickness of 1 μm.

In order to obtain the average grain size and the nitrogen content, the structure was investigated by x-ray diffraction (XRD). We have used for these purposes the Scherrer formula and the relation between the lattice constant and nitrogen concentration.[5] Based on the average lattice parameters, the samples A and B had a nitrogen content of 16%. For the sample deposited on Cu the XRD technique was ineffective because of the superposition of the diffraction peaks of Cu substrate and sample. Because the substrate temperature of −24 °C was almost the same as for the other samples, we expect that the grain size and the nitrogen content will be similar. The surface topography of the samples was analyzed with an atomic force microscope (AFM).

The dc magnetic properties were studied with a vibrating sample magnetometer (VSM). We have measured the high-frequency magnetic response with a single-coil system connected to a network analyzer.[7] An electron-spin-resonance (ESR) setup working in X band (9.4 GHz) was also used.

III. RESULTS

A. Surface morphology

The AFM scans of samples B and C are presented in Figs. 1(a) and 1(b). We have observed that the film surface roughness increases going from sample A (Si-oxide substrate, not shown here) via sample B (organic substrate) to sample C (Cu substrate). The substrate morphology revealed similar features with those of the film surface upon 110-nm deposition of Fe, indicating replication of the substrate topology. This was observed on AFM scans of those regions of the samples which were not covered by the magnetic material due to the substrate holder shadowing effect. The orientation of the coordinate system used here is given in Fig. 2.

Indeed, the height-difference correlation function $g(x) = \langle [h(x)-h(0)]^2 \rangle$ in the fast scan direction was computed (and averaged along the z direction or slow scan direction), where $h(x)$ is the surface height at lateral position x on the surface relative to the mean surface height. A typical example is shown in Fig. 1(c). For a self-affine rough morphology we have[8]

$$g(x) = \rho^2 x^{2H} \quad \text{if } x \ll \xi, \tag{1}$$

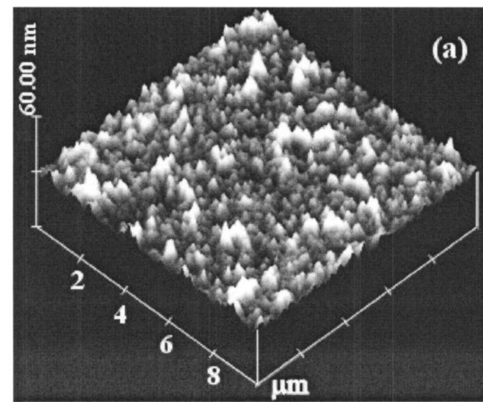

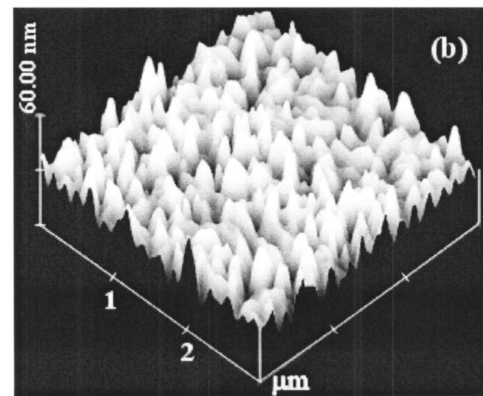

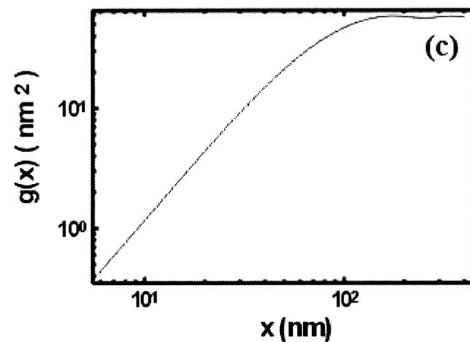

FIG. 1. AFM scans of the samples B (a) and C (b); height difference correlation function corresponding to sample C.

$$g(x) = 2w^2 \quad \text{if } x \gg \xi, \tag{2}$$

with ξ the lateral correlation length, $w = \sqrt{\langle h^2 \rangle}$ the rms roughness amplitude, and $\rho \propto w/\xi^H$ the average local surface slope. Therefore, the rms roughness amplitude w can be obtained from the regime of saturation of $g(x)$ (where its measurement requires a scan size $>10\xi$), while a double log plot at shorter length scales yields the roughness exponent H [Fig. 1(c)]. As H decreases, the surface becomes more irregular (jagged) at short length scales ($x \ll \xi$). Finally, the correlation length ξ is given from the intersection of power-law and saturation lines by $\xi = (2w^2/\rho^2)^{1/2H}$. The measurement of the roughness parameters w, ξ, and H allows further calculation of the demagnetizing factors.

Downloaded 05 Oct 2006 to 129.125.25.39. Redistribution subject to AIP license or copyright, see http://jap.aip.org/jap/copyright.jsp

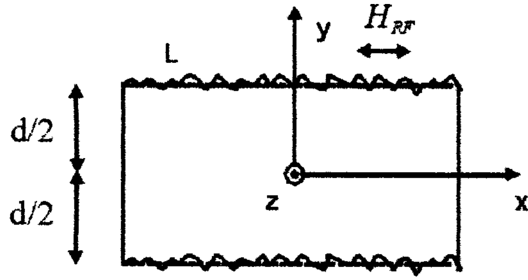

FIG. 2. The cross section of the film lying in the x-z plane; d is the film thickness; L is the film boundary defined by $\pm d/2+h(x,z)$.

The roughness analysis for the sample shown in Figs. 1(b) and 1(c) (Fe/Cu; scan size 3000 nm) yielded $H=0.92\pm0.05$, $w=5.1$ nm, and $\xi=78.2$ nm. For the sample B shown in Fig. 1(a) (Fe–Zr–N/polymer) the rms roughness amplitude is saturated over scan sizes 6000 nm or more due to the presence of the hillocks, yielding $w=2.3$ nm. These hillocks have lateral base dimensions $L\approx400$ nm with average height $\Delta\approx5$ nm and are very likely to dominate magnetic film characteristics. Finally, for the Fe films deposited onto Si oxide the obtained rms roughness amplitude was ≈0.3 nm thus excluding any significant contribution of surface/interface roughness on magnetic properties.

For the film shown in Figs. 1(b) and 1(c) the demagnetizing factors are calculated as follows. If we assume isotropic and translation invariant random roughness in two dimensions, then the average in-plane demagnetizing factor is given by[9]

$$N_{xx}=N_{zz} =\frac{(2\pi)^4}{4dA}\int d^2k[\langle|h_f(k)|^2\rangle+\langle|h_s(k)|^2\rangle -2e^{-dk}\langle h_f(k)h_s(k)\rangle]k \quad (3)$$

with $h_f(k)$ and $h_s(k)$, respectively, the two-dimensional Fourier transform of the film surface and substrate height fluctuations. A is the average macroscopic flat surface area. Note that the diagonal components of the demagnetizing factor are determined by the relations $N_{xx}=N_{zz}$ (isotropic roughness) and $N_{xx}+N_{yy}+N_{zz}=1$. The approximation, which we make, is that everywhere the spins are parallel. For conformal to substrate film surface roughness, or $h_f(k)\equiv h_s(k)$, Eq. (3) yields

$$N_{xx}=\frac{(2\pi)^4}{2dA}\int d^2k\langle|h_f(k)|^2\rangle k(1-e^{-dk}). \quad (4)$$

In order to calculate the demagnetizing factor we assume a simple Lorentzian model for the roughness spectrum[10] $\langle|h_f(k)|^2\rangle$

$$\langle|h_f(k)|^2\rangle=\frac{A}{(2\pi)^5}\frac{w^2\xi^2}{(1+ak^2\xi^2)^{I+H}} \quad (5)$$

with $a=(1/2H)[1-(1+aQ_c^2\xi^2)^{-H}]$ if $0<H<1$ (power-law roughness), and $Q_c=\pi/a_0$ with a_0 of the order of atomic dimensions. For other self-affine roughness correlation models see also Ref. 11.

For the roughness parameters $H=0.92$, $w=5.1$ nm, and $\xi=78.2$ nm of the sample C deposited onto Cu [Figs. 1(b) and 1(c)] we obtain the in-plane demagnetizing factors $N_{xx}=N_{zz}=3.6\times10^{-3}$. Furthermore, for sample B shown in Fig. 1(a) the demagnetizing factor was estimated using a different approach since the surface has a different hillock configuration. Here we can approximate the large wavelength features with uniform magnetized ellipsoids having the long axis equal with L and the short axis equal with Δ. In this case we obtain (Ref. 12) $N_{xx}=N_{zz}\cong1\times10^{-3}$.

B. Magnetic characterization

We present in Fig. 3 the hysteresis loops of the samples measured with applied field, H_{dc}, parallel and perpendicular to the easy axis (EA). In the coordinate system chosen the Oy axis is perpendicular to the surface, EA is along the Oz axis and the rf field is along Ox. All samples measured in the EA orientation had values of the remanent magnetization almost equal to saturation values. This shows that a stable single-domain magnetic structure is formed even when the external field is zero. The initial permeability is larger than $N_{xx}^{-1}=N_{zz}^{-1}$, i.e., the system does not form domains in order to keep the internal field zero, which would minimize the magnetostatic energy. The reason for this behavior lies on the fact that the spins cannot follow all the topography variations due to the significant strength of the exchange interactions. Moreover, the values of the coercive fields for the hard axis orientations in Figs. 3(b) and 3(c) are rather remarkable. Indeed, because these values are close to the easy axis orientation, we associate a noncoherent spin rotation in the case of magnetization reversal along the hard axis orientation.

In principle the uniaxial anisotropy field, H_K, can be extracted from the hysteresis loops measured in the hard direction. Its origin is in a preferential distribution of the nitrogen atoms in the octahedral interstitial positions of the cubic lattice.[13] We could estimate reliably H_K in this way only for sample A, which has a coercive field of about 1 Oe. For samples B and C, where the coercivity is much higher, we estimate that H_K does not exceed 25 Oe. A better estimation of H_K field was performed using FMR at 9.4 GHz (see Table II). Figure 4 shows an example of the X-band measurements. As pointed out by Oates *et al.*[14] the output signal of an ESR spectrometer is composed of absorption and dispersion lines. In the ideal case only the absorption line should be observed. By introducing a dispersion component we can fit the signal correctly and determine the resonance field H_R together with the field linewidth ΔH. The analysis can be performed using the following formula:

$$y=a\left(\frac{H_R-H}{\Delta H_R}\right)+9b-3b\left(\frac{H_R-H}{\Delta H_R}\right)^2 \times\left[3+\left(\frac{H_R-H}{\Delta H_R}\right)^2\right]^{-2}, \quad (6)$$

where y is the field derivative of the absorbed power during FMR process, the coefficients a and b are the amplitudes of the absorption and dispersion signals, respectively. Because the field derivative y is measured in arbitrary units, the values of a and b are difficult to be related directly with a physical parameter like the permeability. However, here we are only interested in a correct description of the spectrum

Downloaded 05 Oct 2006 to 129.125.25.39. Redistribution subject to AIP license or copyright, see http://jap.aip.org/jap/copyright.jsp

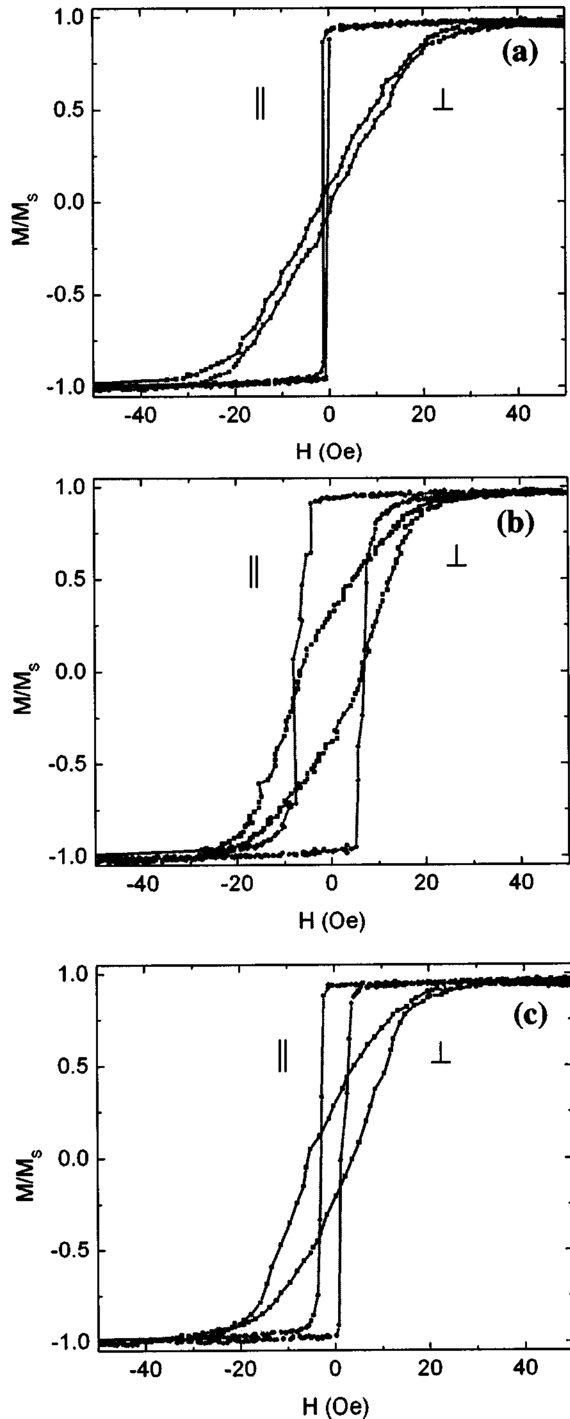

FIG. 3. Hysteresis loops of the samples A (a), B (b), and C (c); measurements performed parallel and perpendicular to the easy axis.

shape in order to extract the linewidth and the resonance field values. An example of such a fit is presented in Fig. 5. As already mentioned, H_K was calculated from the half of the difference between H_R obtained with Eq. (6) for the situation when the external field is oriented in the plane of the sample perpendicular to EA and parallel to EA, see Fig. 4. The values of $\Delta H/2$ corresponding to the FMR lines in Fig. 5 are also included in Table II.

The values of $4\pi M_S$ as given in Table II are calculated assuming[15] $g=2.1$ for all the samples used in the present study. In fact, for the estimation of $4\pi M_S$ we have taken into account not only the X-band measurements, but also the frequency-dependent permeability (see later). Since all samples were deposited in almost the same sputtering conditions, it is expected not to be a significant variation of the saturation magnetization M_S.

The frequency-dependent permeability of the samples is presented in Fig. 6. A clear difference can be observed between the sample deposited on Si and the samples deposited on the organic and Cu-covered substrates. While sample A presents a relatively sharp resonance with a $\Delta\omega \cong 520$ MHz, the resonances in samples B and C were very broad, with a frequency width half maximum (FWHM) larger than 1 GHz. This increase of the linewidth is accompanied by an increase of the average resonance frequency, corresponding to the zero crossing of the real part of the permeability μ'. It is evident that a correlation exists between the sample roughness and the high-frequency response.

1. Method 1

As a first method of analysis, we suppose that in samples B and C the local demagnetizing field is oscillating from one region to another and has the following position dependence: $H_{dz}=H_0\cos(kz)=H_0\cos(\theta)$ where $\theta\epsilon[0,\pi]$ and $2\pi/k$ is appreciably larger than the correlation length ξ. For coherent rotation of spins, the dynamics of the system can be reasonably well described by the Landau–Lifshitz equation.[16] Details about the solution of this equation are given elsewhere.[17,18] We note that no eddy current effects are expected because the chosen film thickness is much smaller than the skin depth for our N-rich nanocrystalline thin films. Furthermore, in order to fit our frequency-dependent spectra, we have considered the total local field

$$\mathbf{H}_T=\mathbf{H}_{\rm dc}+\mathbf{H}_{\rm ef}(t)+\mathbf{H}_K-\mathbf{H}_{\rm dem}+\mathbf{H}_d+\mathbf{H}_{\rm Shift}, \tag{7}$$

where $\mathbf{H}_{\rm dem}=(0,4\pi M_S,0)$ is the demagnetizing field in the absence of surface roughness and $\mathbf{H}_d=(H_{dx},H_{dy},H_{dz})$ is the local demagnetizing field, which should not be confused with the average value calculated on the basis of the demagnetizing factor coefficients (N_{xx}, N_{yy}, and N_{zz}). $\mathbf{H}_{\rm Shift}$ is an extra field needed to obtain a good fit of the experimental data. Its origin is discussed in the next section and is related to the material nanostructure. The frequency-dependent magnetic response of the system is obtained by calculating the envelope of the permeability curve $\mu=\mu(\theta)$ over a period of the oscillating $\mathbf{H}_d$.

For this analysis we have chosen $n=20$ equidistant values of θ and the same damping constant $\alpha_{\rm frequency}$ for each individual spectrum. Since $\alpha_{\rm frequency}$ does not influence significantly the FMR frequency, its effect on the simulated spectra is only to modify the FMR linewidth of the individual spectrum. An increase of n did not change the values of $\alpha_{\rm frequency}$ as a free parameter in the fitting procedure. Figure 6 presents the fits based on this model of H_d. In Table II we present the results of this analysis. We see that the amplitude of the demagnetizing field H_d increases clearly with the roughness. Like $\mathbf{H}_0$, $\mathbf{H}_{\rm Shift}$ correlates with the roughness of the films and will be subject of discussion in the next section. Note also that in Table II we use two different notations for the damping parameter: one as determined from the

Downloaded 05 Oct 2006 to 129.125.25.39. Redistribution subject to AIP license or copyright, see http://jap.aip.org/jap/copyright.jsp

TABLE II. Magnetic parameters: anisotropy field measured with VSM ($H_{K\text{-VSM}}$) and X-band FMR ($H_{K\text{-FMR}}$), H_r is the average resonance field and ΔH_{FMR} is the linewidth from X-band measurement, and f_R is the resonance frequency obtained from permeability spectra.

Sample	A	B	C
$H_{K\text{-VSM}}$ (Oe)	23	<25	<25
$H_{K\text{-FMR}}$ (Oe)	23	13	29
$H_r=(H_{r\perp}+H_{r\parallel})/2$ (Oe)	625	613	578
ΔH_{FMR} (Oe)	14.5	35	92
$4\pi M_S$ (kG)	15.6	15.4	16
f_R (GHz)	1.95	2.33	2.92
H_K+H_{Shift} (Oe)	28	39	54
H_0 (Oe)	0	24.6	44
α_{field}	0.0023	0.0054	0.014
$\alpha_{\text{frequency}}$	0.01	0.023	0.025
$N_{xx}4\pi M_S$ (Oe)	⋯	15	55

frequency-dependent measurements (presented above) and a second one for the field-dependent spectra (α_{field}). This is made in order to stress the distinction between the frequencies and magnetic fields specific for each type of measurement.

2. Method 2

We can also estimate the distribution of local demagnetizing fields by transforming the spectra $\mu=\mu(f)$ into $\mu=\mu(H_{\text{eff}})$ via the dispersion relationship

$$f_{H_{\text{rf}}\parallel HA}=\frac{\gamma}{2\pi}\sqrt{4\pi M_S H_{\text{eff}}}, \tag{8}$$

where $\gamma=g\mu_B/\hbar$ is the gyromagnetic ratio and μ_B is the Bohr magnetron. The effective field acting on the spins is given by $H_{\text{eff}}=H_k+H_{\text{Shift}}+H_d$. If we neglect the intrinsic linewidth with respect to the inhomogeneous broadening of the resonance line, the curve of μ' versus H_{eff} reflects the distribution of the local-fields H_d (Fig. 7). This is a reasonable assumption, because the linewidth for sample A is much narrower than for B and C. On the other hand, for a successful fit assuming a sinusoidal wave variation of H_d we had to introduce a much larger homogeneous linewidth for samples B and C. Thus, we may overestimate the width of the distribution by this method. However, the large homogeneous linewidth used in method 1 may also be (partly) the consequence of the fact that the local-field distribution is assumed to be sinusoidal. These results show some evidence for an increased homogeneous linewidth for samples B and C.

At any rate, both methods 1 and 2 gave rather comparable results. We see that the values of the half linewidths (32 and 54 Oe) are very close to those of $\mathbf{H}_0$ presented in Table II. We also noticed that the average field was much larger than the anisotropy H_K.

IV. DISCUSSION

Based on the interpretation given in Sec. III, we summarize the effects observed on the FMR absorption line: (i) the line asymmetry, (ii) the line position, and (iii) the homogenous linewidth as observed in the damping parameter.

Line shape. Our permeability measurements clearly show that there exists an asymmetric distribution of resonance frequencies. We ascribe this to a distribution in local demagnetizing fields, due to the roughness of both film interfaces. In comparing with the AFM analysis, we have to realize that due to the strong exchange interactions, the spins are coupled over regions with an in-plane area proportional to the square of the magnetic correlation length ξ_m. In the context of the random anisotropy model, for pure nanocrystalline Fe (Ref. 19), ξ_m increases significantly from 40 up to 120 nm with the decrease of the grain size from 20 to 10 nm. Although the average grain size of our samples is smaller, we expect a magnetic correlation length in this range of magnitude for the samples B and C. The reason is the presence of the dipolar interactions due to the surface morphology. Only the structural irregularities larger than ξ_m will lead to variations in the resonance frequency of the local magnetization, i.e., to inhomogeneous line broadening.

Although a quantitative comparison is difficult, we expect that the average demagnetizing field $H_{zz}=N_{zz}4\pi M_S$ as calculated from the AFM profiles will be close to the half-width of the local-field distribution (method 2) or, alternatively, to the amplitude of the sinusoidal variation H_0 (method 1). For sample B, the size of the hillocks $L\cong 400$ nm is much longer than the magnetic correlation length, so that $H_{zz}=N_{zz}4\pi M_S\cong 15$ Oe is the appropriate estimate for the interface roughness. Given the very rough nature of this estimate, this is in agreement with the permeability estimates: 25 Oe (method 1) and 32 Oe (method 2). For sample C we have a lateral correlation length $\xi=78$ nm. It turns out that limiting the integration in Eq. (4) to $k_{\max}=2\pi/\xi_m$ has a negligible influence on the value of N_{zz}. The value $N_{zz}4\pi M_S=55$ Oe compares well with the permeability estimates: 44 and 54 Oe, respectively.

Line shift. Recently, Arias and Mills[20] proposed a model for thin films, based on scattering of the normal mode by bumps and pits on the sample surface or the sample/substrate interface. According to their interpretation, the shift effect may occur only if there is a *preferential* orientation of the surface imperfections. Contrary to this, we clearly observe a FMR line shift but we have no evidence for a preferential orientation of the surface defects. If we assume that the de-

Downloaded 05 Oct 2006 to 129.125.25.39. Redistribution subject to AIP license or copyright, see http://jap.aip.org/jap/copyright.jsp

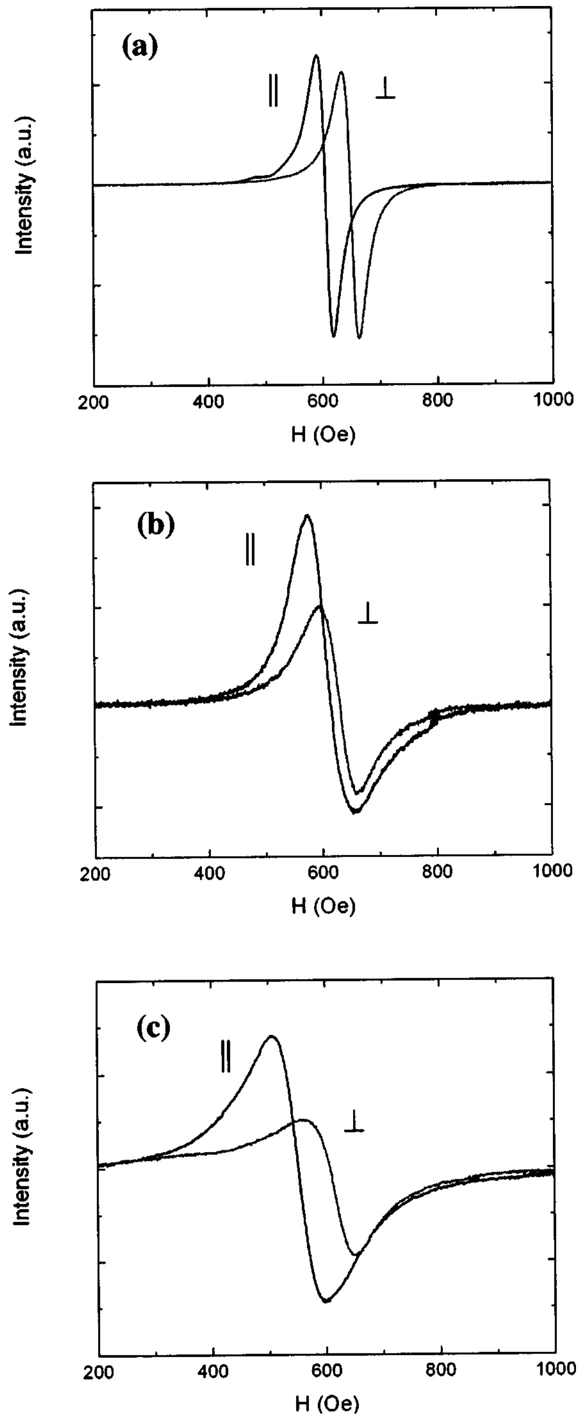

FIG. 4. ESR spectra of samples A (a), B (b), and C (c) measured H_{dc} parallel and perpendicular to the EA; in-plane geometry.

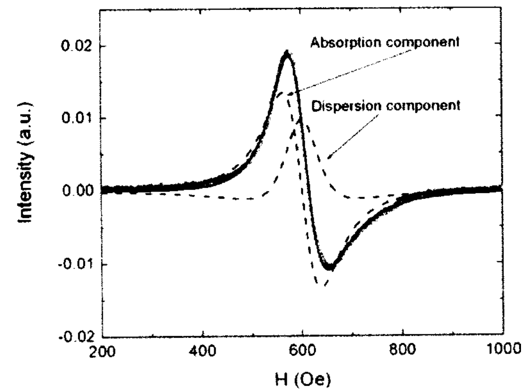

FIG. 5. ESR measurement for sample B: Experimental data is represented by circles, the absorption and dispersion components are indicated by arrows and the fit of the experimental data is represented by the continuous line.

magnetizing fields H_{xx} and H_{zz} are equal due to the random character of the surface imperfections, their contribution in the general expression of the FMR frequency will cancel out

$$f_R = \frac{\gamma}{2\pi}[H_k + (N_{xx} - N_{zz})4\pi M_S]^{1/2} \times [H_k + (N_{yy} - N_{zz})4\pi M_S]^{1/2}. \quad (9)$$

A possible origin of the FMR frequency shift can be the magnitude variation of the magnetization due to the existence of intergranular regions[21] (equivalent with variations of crystal periodicity). The perpendicular magnetization component M_x can be associated with a magnetostatic energy density $\langle (M_x - M_{av,x})^2 \rangle$. Applying the simple model of Jamet and Malozemoff,[22] which assumes a sinusoidal variation of the magnetization with amplitude M_1, we estimate $M_1 \approx 4 \times 10^2$ G for sample A and 9×10^2 G for samples B and C. These values are 2.5% and 6%, respectively, of the saturation magnetization. Probably the rougher surface topography of substrates B and C leads to larger density magnetization fluctuations.

Spin-wave excitation. The damping constants as determined from the X-band measurements (α_{field}) and from the permeability spectra ($\alpha_{\text{frequency}}$) are presented in Table II. For the same sample the values calculated from the permeability spectra are larger than those obtained from the FMR measurements. (In fact the difference is even more pronounced, because we did not take inhomogeneous broadening into account in the X-band measurements, whereas we did so in the permeability analysis via the parameter H_0). In addition we observe that $\alpha_{\text{frequency}}$ and α_{field} increase with the sample roughness.

In the framework of the two-magnon scattering process, the homogenous broadening of the resonance line is associated with the presence of spin waves with the same energy as the uniform precession mode. The uniform precession mode is scattered by randomly distributed inhomogeneities into these spin-wave modes. As a consequence the damping parameter α will increase (above its intrinsic value) with the number and the volume of the magnetic inhomogeneities. This interpretation is widely accepted.[23] In our case the structural imperfections in the bulk and the surface can be considered as scattering centers in the two-magnon process. For H_{dc} oriented in the plane the uniform FMR mode is degenerate, where the whole spin-wave band is reflected in the damping parameter evolution from small values for sample A to presumably very large values for sample C.

V. CONCLUSIONS

We have demonstrated that the high-frequency magnetic response can be influenced by changes of the substrate roughness obtaining a "tunable" magnetic material with high

Downloaded 05 Oct 2006 to 129.125.25.39. Redistribution subject to AIP license or copyright, see http://jap.aip.org/jap/copyright.jsp

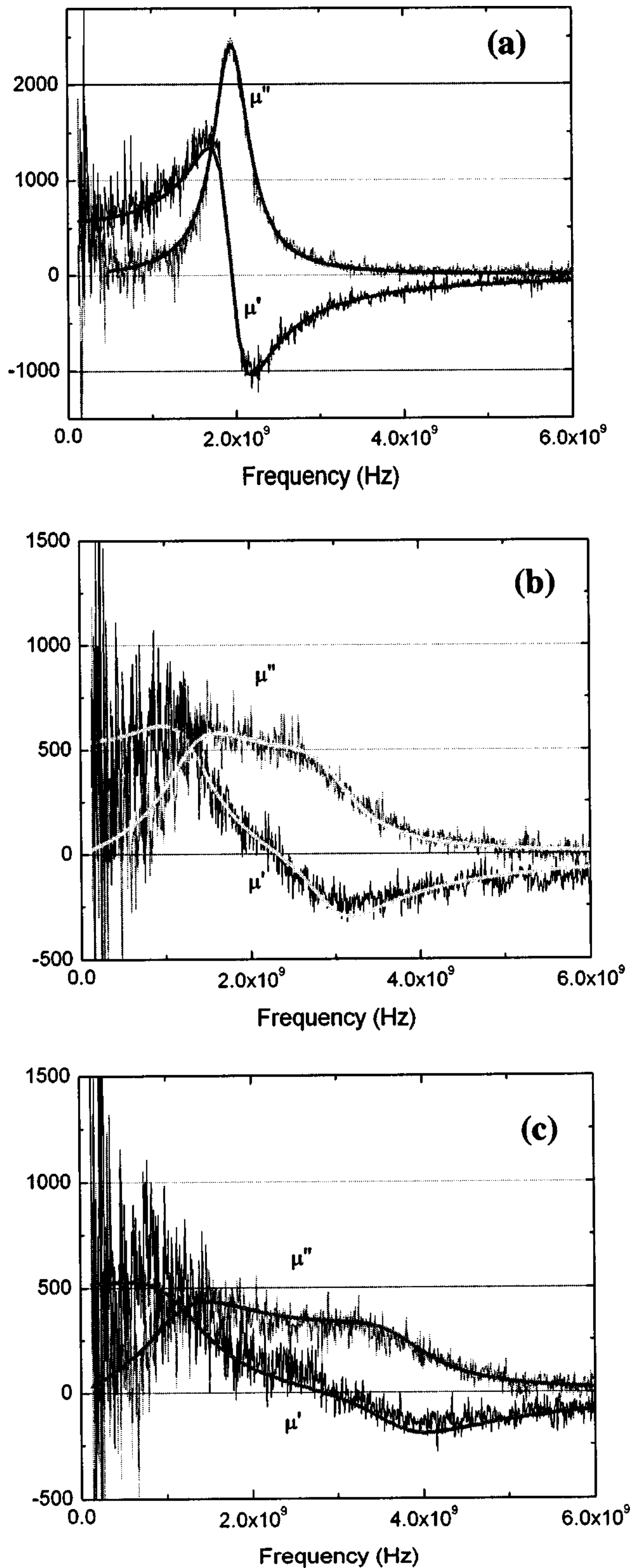

FIG. 6. Measurement and simulation of real and imaginary part of the complex permeability for samples A (a), B (b), C (c).

saturation magnetization. It turns out that both the shift and the broadening of the resonance line can be understood through the influence of the film interface roughness. The estimations of the demagnetizing field as calculated from the analysis of the AFM scans are reasonably close to the values obtained from the FMR frequency-dependent measurements.

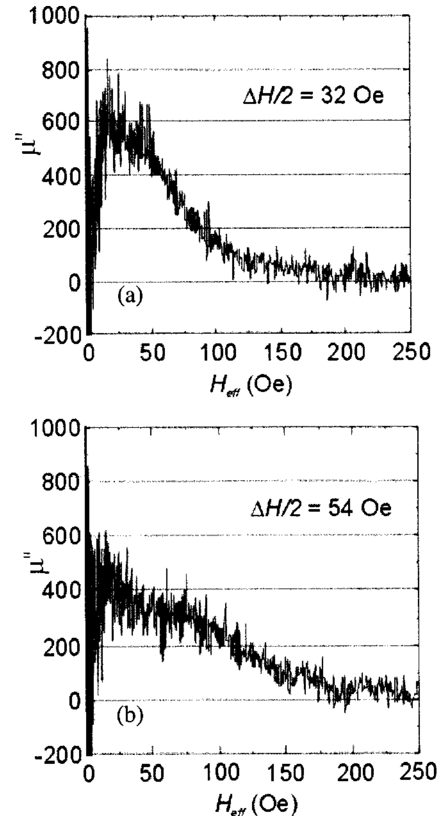

FIG. 7. $\mu''=\mu''(H_{\mathrm{eff}})$ obtained directly from the dispersion relationship (a) for sample B and (b) for sample C.

A possible route of further investigations is to continue this study for thin films deposited on patterned substrates obtained, for instance, by laser interference lithography.[24] In this way the magnitude of the local demagnetizing field can be controlled in an easier manner. Complementary, FMR field dependence measurements realized with the external applied field oriented perpendicular to the sample surface would be quite interesting. This is because in such geometry the two-magnon scattering process is absent, and as a result it could yield a more definite proof why we have an unusual large damping constant in our samples.

ACKNOWLEDGMENTS

The authors would like to thank Professor H. W. den Hartog for helpful discussions and J. F. Golstein for assistance in performing the high-frequency measurements. This work was supported by Grant No. GWN 4561 of the Dutch Technology Foundation (STW) and the “Prioriteitsprogramma Materiaalonderzoek (PPM).”

[1]M. Yamaguchi *et al.*, J. Appl. Phys. **85**, 7919 (1999).
[2]M. Yamaguchi, M. Baba, and K. I. Arai, IEEE Trans. Microwave Theory Tech. **49**, 2331 (2001).
[3]G. Herzer, IEEE Trans. Magn. **26**, 1397 (1990).
[4]R. Alben, J. Appl. Phys. **49**, 1653 (1978); E. M. Chudnovsky, W. M. Saslow, and R. A. Serota, Phys. Rev. B **33**, 251 (1986).
[5]A. R. Chezan, Ph.D. thesis, University of Groningen, The Netherlands, 2003.
[6]J. F. Bobo, H. Chatbi, M. Vergnat, L. Hennet, O. Lenobe, P. Bauer, and M. Piecuch, J. Appl. Phys. **77**, 5309 (1995).
[7]D. Pain, M. Ledieu, O. Acher, A. L. Adenot, and F. Duverger, J. Appl. Phys. **85**, 5151 (1999).

Downloaded 05 Oct 2006 to 129.125.25.39. Redistribution subject to AIP license or copyright, see http://jap.aip.org/jap/copyright.jsp

[8]J. Krim and G. Palasantzas, Int. J. Mod. Phys. B **9**, 599 (1995); *Characterization of Amorphous and Crystalline Rough Surfaces—Principles and Applications*, Experimental Methods in the Physical Science Vol. 37, (Academic, New York, 2000); P. Mearkin, *Fractals, Scaling, and Growth Far from Equilibrium* (Cambridge University, Cambridge, 1998); T. Halpin-Heally, Phys. Rep. **254**, 215 (1995).
[9]Y. P. Zhao, G. Palasantzas, G. C. Wang, and J. Th. M. De Hosson, Phys. Rev. B **60**, 1216 (1999); G. Palasantzas, J. Appl. Phys. **86**, 2196 (1999).
[10]G. Palasantzas, Phys. Rev. B **48**, 14472 (1993); G. Palasantzas, *ibid.* **49**, 5785 (1994).
[11]G. Palasantzas and J. Krim, Phys. Rev. B **48**, 2873 (1993); G. Palasantzas, Phys. Rev. E **49**, 1740 (1994); S. K. Sinha, E. B. Sirota, S. Garoff, and H. B. Stanley, Phys. Rev. B **38**, 2297 (1988); H. N. Yang and T. M. Lu, Phys. Rev. E **51**, 2479 (1995).
[12]E. Schlömann, J. Appl. Phys. **41**, 1617 (1970).
[13]E. van de Riet, W. Klaassens, and F. Roozeboom, J. Appl. Phys. **81**, 350 (1997).
[14]C. J. Oates, F. Y. Ogrin, S. L. Lee, P. C. Riedi, G. M. Smith, and T. Thompson, J. Appl. Phys. **91**, 1417 (2002).
[15]S. Chikazumi, *Physics of Ferromagnetism* (Oxford University, New York, 1997).
[16]L. Landau, Phys. Z. Sowjetunion **8**, 163 (1935).
[17]E. van de Riet, W. Klaassens, and F. Roozeboom, J. Appl. Phys. **81**, 806 (1997).
[18]J. Huijbregtse, F. Roozeboom, J. Sietsma, J. Donkers, T. Kuiper, and E. van de Riet, J. Appl. Phys. **83**, 1569 (1998).
[19]J. Loffler, H. B. Braun, and W. Wagner, Phys. Rev. Lett. **85**, 1990 (2000).
[20]R. Arias and D. L. Mills, Phys. Rev. B **60**, 7395 (1999).
[21]C. B. Craus, A. R. Chezan, N. G. Chechenin, D. D. Boerma, and L. Niesen, Phys. Rev. B (unpublished).
[22]J. P. Jamet and A. P. Malozemoff, Phys. Rev. B **18**, 75 (1978).
[23]M. Sparks, R. Loudon, and C. Kittel, Phys. Rev. **122**, 791 (1961).
[24]J. C. Lodder, M. A. M. Haast, and L. Abelmann, *Magnetic Storage Systems Beyond 2001* (Kluwer Academic Publishers, Dordrecht, The Netherlands, 2001), p. 117.

Downloaded 05 Oct 2006 to 129.125.25.39. Redistribution subject to AIP license or copyright, see http://jap.aip.org/jap/copyright.jsp